Dynamic range and linearity trade-off in detectors for interferometric radiometers

F. Torres, N. Duffo, I. Corbella, A. Camps,
M. Vall.llossera and L. Sagués

The dynamic range and error performance of the diode power detector used to denormalise the digital correlations in interferometric radiometers is analysed by means of a second-order model of the diode response. This gives an easy method to establish system dynamic range as a trade-off between both the error contribution of measurement uncertainty and diode nonlinearity. The method is illustrated by analysing the power measurement system of the MIRAS-SMOS instrument.

Introduction: This Letter presents a simplified trade-off analysis of the dynamic range and error performance of the power measurement system (PMS) in each microwave imaging radiometer with aperture synthesis (MIRAS) [1], which is the single payload of the ESA-SMOS mission [2]. MIRAS consists of a Y-shape interferometric radiometer formed by 69 receivers placed along the arms. Cross-correlation of the signals collected by all receiver pairs gives a sample of the so-called visibility function, and the brightness temperature map is obtained, in a first approximation, by an inverse Fourier transform. Since the instrument uses 1-bit digital correlators, it actually measures normalised cross-correlations. Hence, the equivalent system temperature at the input of each receiver must be measured in order to denormalise each visibility sample prior to inversion [3]. These measurements are performed by means of a PMS placed in each receiver in the signal path prior to the correlator unit.

Four point measurement technique: A simplified block diagram of a PMS is shown in Fig. 1. When an equivalent system temperature T_{sys} is driven to its input, the measured voltage is given by

$$V = V_{off} + GT_{sys} = V_{off} + G(T_{ext} + T_r) \qquad (1)$$

where a linear model of the diode power detector has been taken into account, T_r is the receiver equivalent noise temperature, and T_{ext} stands for the equivalent external temperature. In the measurement mode, this one is given by the equivalent antenna temperature T_A, while in calibration mode it is given by the so-called COLD and HOT temperatures T_C and T_H. The overall system gain can be switched between two values G and G/L ($L > 1$) by means of an attenuator placed in the signal path at a point that it does not affect T_r [4]. For the different combinations of T_C, T_H and L the following set of voltage measurements are obtained:

$$\begin{aligned} V_1 &= V_{off} + G(T_C + T_r) \quad & V_2 &= V_{off} + G(T_H + T_r) \\ V_3 &= V_{off} + \frac{G}{L}(T_C + T_r) \quad & V_4 &= V_{off} + \frac{G}{L}(T_H + T_r) \end{aligned} \qquad (2)$$

From (2) the PMS unknown parameters V_{off} and G are readily obtained as

$$V_{off} = \frac{V_2 V_3 - V_1 V_4}{(V_2 - V_4) - (V_1 - V_3)} \quad \text{and} \quad G = \frac{V_2 - V_1}{T_H - T_C} \qquad (3)$$

and the required equivalent system temperature T_{sysA} is estimated as:

$$T_{sysA} = T_A + T_r = \frac{V_A - V_{off}}{V_2 - V_1}(T_H - T_C) \qquad (4)$$

where V_A is the PMS voltage reading in measurement mode. The main advantage of this approach lies in the fact that T_H and T_C appear exclusively in differential mode. This is specially important because T_H and T_C are injected by a noise source (NS) simultaneously to a large set of receivers via a noise distribution network (NDN) [1, 3] (Fig. 1). T_H and T_C are also injected through the same NDN to a noise injection radiometer (NIR) in order to have absolute knowledge of both T_H and T_C. Hence, noise contribution of the NDN itself is removed because of the differential mode ($T_H - T_C$).

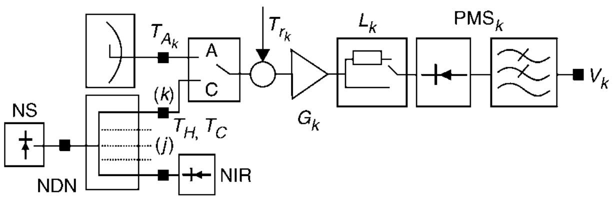

Fig. 1 *Simplified block diagram of PMS and two-level noise injection network*

Effect of measurement uncertainties: There are two main error sources of T_{sysA}: PMS nonlinearity and measurement uncertainty in V, T_H, and T_C. The impact of the measurement uncertainty is directly related to system dynamic range, which can be defined as the product $DR = Y \cdot L$, where Y is the ratio of system temperatures in HOT and COLD modes: $Y = (T_H + T_r)/(T_C + T_r)$. Note that the actual value L of the attenuator is not required to estimate T_{sysA}, however it has a large impact in the estimation of V_{off}, since the values into parenthesis in (3) tend to zero as L tends to 1 (0 dB). Fig. 2*a* gives the standard deviation of the fractional error in the estimation of T_{sysA} (σ_{TsysA} in %) against L (*x*-axis) and Y (parametric curves for $Y = 2, 4, 8, 16$). The fractional standard deviation of the PMS voltage readings is $\sigma_V = 0.1\%$ and the uncertainty in the calibration temperatures are $\sigma_{Th,Tc} = 0.1\%$. The plots in Fig. 2*b* do not take into account diode nonlinearity which is discussed in the following Sections. With this assumption, it is clear that both Y and L should be as large as possible in order to reduce the effect of measurement uncertainty.

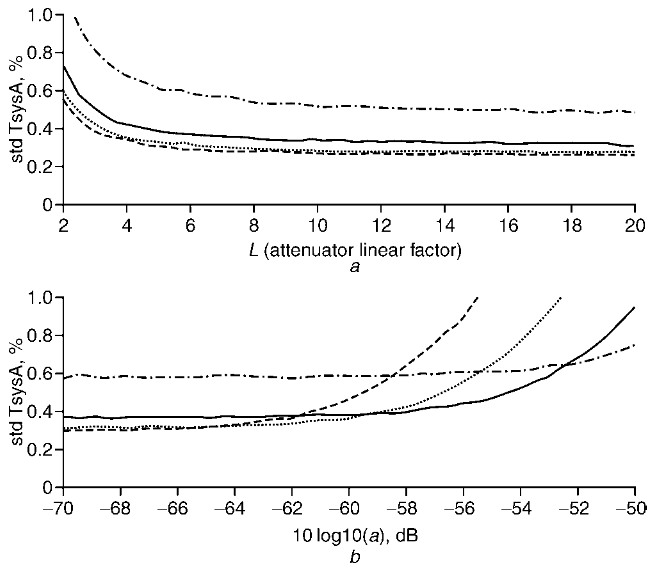

Fig. 2 *Error in estimation of T_{sysA} against L and linearity*

a Against L
b Against linearity
$\sigma_V = \sigma_{Th,Tc} = 0.1\%$, $L = 6$
$Y = 2$ (· – · –)
$Y = 4$ (——)
$Y = 8$ (· · ·)
$Y = 16$ (-----)

Power detector characterisation: Power measurement is implemented by means of a Schottky diode detector followed by a lowpass filter as integrator. To test the method, four detectors have been characterised. Voltage readings range from 170 to 1150 mV for equivalent system temperatures ranging from 475 to 3950K. Fig. 3*a* gives the error of measured data when fitted to a linear model (1)—in a least squares sense. The effect of nonlinearity is clearly seen, giving a standard deviation from the linear model of ~0.4%. To asses the impact of nonlinearity in the detector performance, data has been fitted to a second-order model given by

$$V_k = V_{offk} + G_k T_{sys} + a_k T_{sys}^2 \qquad (5)$$

The parameter a_k gives the degree of nonlinearity of the PMS numbered 'k'. Fig. 3*b* represents the error of measured data in relation to the second-order model. Now the standard deviation of the error is

~0.06%, clearly due to measurement uncertainty. Hence, PMS nonlinearity can be well represented by a second-order model with mean $\langle a \rangle = 1.6 \cdot 10^{-6}$ mV/K^2, $\langle G \rangle = 0.292$ mV/K, $\langle V_{off} \rangle = 75.82$ mV and standard deviation $\sigma_a = 3.0 \cdot 10^{-7}$ mV/K^2, $\sigma_G = 0.032$ mV/K and $\sigma_{Voff} = 6.57$ mV. Data from PMS2 have been discarded since it clearly presents a bad performance.

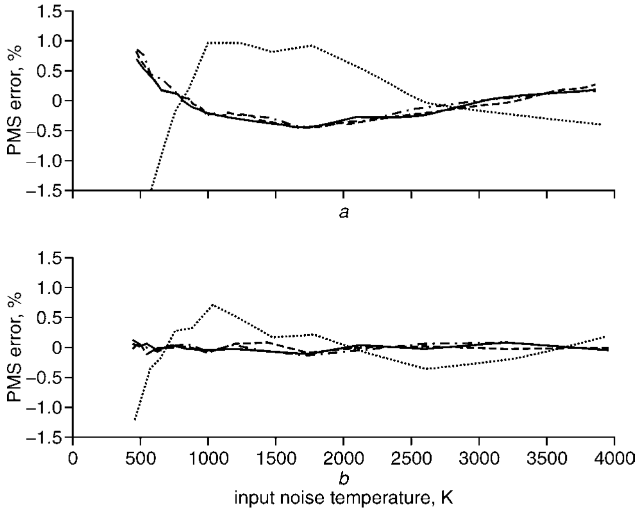

Fig. 3 *PMS error: linear model and quadratic model*

a Linear model
b Quadratic model
Measured units:
PMS_1 (——)
PMS_2 (· · ·)
PMS_3 (· – · –)
PMS_4 (– –)

Effect of nonlinearity and dynamic range trade-off: Fig. 2*b* shows the standard deviation of the estimated system temperature, against the second-order effect setting the attenuator to $L = 6$ to keep a moderate dynamic range. The actual PMS voltage readings have been simulated by means of the second-order model, while the estimated T_{sysA} has been obtained through the linear model in (2). The x-axis represents the effect of the second-order parameter a_k—(5) ranging from −70 to −50 dB, being the actual value for the measured set of samples of $10 \log(a_k) = -58$ dB. For low values of a_k Fig. 2*b* shows that the dominant contribution to the error in T_{sysA} is given by measurement uncertainty (the same value shown in Fig. 2*a* for $L = 6$). However, as nonlinearity increases, the effect of nonlinearity becomes the dominant effect, which is highly dependent on the value of Y. In this particular case, a trade-off value for Y that minimises the error is given by $Y = 4$. Optimum dynamic range becomes $DR = 24$ (13.8 dB) giving equivalent input temperatures at the receiver front end of $T_{\text{sysmin}} = 78$K and $T_{\text{sysmax}} = 1872$K with associated PMS voltage readings of $V_{\min} = 98.6$ mV and $V_{\max} = 628.05$ mV.

Conclusion: A second-order model of a diode power detector provides an easy way to determine the optimum system dynamic range in the MIRAS-SMOS interferometric radiometer as a trade-off between both the error contribution of measurement uncertainty and diode nonlinearity.

Acknowledgments: This work is financed by the Spanish MCYT and EU FEDER funds under project TIC2002-04451-C02-01 and EADS CASA Espacio, under the SMOS PLM project.

18 September 2003
Electronics Letters Online No: 20031164
DOI: 10.1049/el:20031164

F. Torres, N. Duffo, I. Corbella, A. Camps and M. Vall.llossera (*Department of Signal Theory and Communications, Polytechnic University of Catalonia, Barcelona, Spain*)

E-mail: xtorres@tsc.upc.es

L. Sagués (*Space Department, Mier Comunicaciones SA, La Garriga, Spain*)

References

1 MARTIN-NEIRA, M., and GOUTOULE, J.M.: 'A two-dimensional aperture synthesis radiometer for soil moisture and ocean salinity observations', *ESA Bull.*, 1997, **92**, pp. 95–104
2 SILVESTRINI, P., *et al.*: 'ESA's second Earth Explorer Opportunity Mission: The Soil Moisture and Ocean Salinity Mission—SMOS', *IEEE Geosci. Remote Sens. Newsl.*, March 2001
3 TORRES, F., *et al.*: 'On board phase and modulus calibration of large aperture synthesis radiometers: study applied to MIRAS', *IEEE Trans. Geosci. Remote Sens.*, 1996, **34**, (4), pp. 1000–1009
4 PIIRONEN, P.: 'PMS offset determination using an IF attenuator'. Technical Note 14629/00/NL/SF, ESA-ESTEC, Holland, June 2002